Solid-State ^{13}C NMR Reveals Effects of Temperature and Hydration on Elastin

Ashlee Perry, Michael P. Stypa, Brandon K. Tenn, and Kristin K. Kumashiro
Department of Chemistry, University of Hawaii, Honolulu, Hawaii 96822 USA

ABSTRACT Elastin is the principal protein component of the elastic fiber in vertebrate tissue. The waters of hydration in the elastic fiber are believed to play a critical role in the structure and function of this largely hydrophobic, amorphous protein. ^{13}C CPMAS NMR spectra are acquired for elastin samples with different hydration levels. The spectral intensities in the aliphatic region undergo significant changes as 70% of the water in hydrated elastin is removed. In addition, dramatic differences in the CPMAS spectra of hydrated, lyophilized, and partially dehydrated elastin samples over a relatively small temperature range (−20°C to 37°C) are observed. Results from other experiments, including ^{13}C T_1 and ^1H $T_{1\rho}$ measurements, direct polarization with magic-angle spinning, and static CP of the hydrated and lyophilized elastin preparations, also support the model that there is significant mobility in fully hydrated elastin. Our results support models in which water plays an integral role in the structure and proper function of elastin in vertebrate tissue.

INTRODUCTION

Elastin is the principal protein component of the elastic fiber found in vertebrate tissue (Rosenbloom et al., 1993). Its amino acid composition is dominated by the presence of residues with significant hydrophobic character. Glycine, alanine, valine, and proline make up over 80% of the typical elastin sample, and these amino acids are usually found in repeating, polypeptidyl motifs. Many of the alanines are also found in the cross-linking regions. Due to the hydrophobic nature of elastin, this amorphous, cross-linked protein is insoluble in water and many organic solvents. For these reasons, the high-resolution structure has not been solved by x-ray crystallography or solution NMR. Recently, this laboratory has published a study utilizing methods in high-resolution solid-state NMR to characterize lyophilized α-elastin, an acid-solubilized form of elastin, from normal and under-cross-linked pig aortas (Kumashiro et al., 2001). These results indicated that the overall structures of normal and under-cross-linked elastin were similar but that there was more mobility in the normal protein. In general, our previous work suggested that there were some defined structural elements in elastin. However, the proper function of elastin was correlated with significantly high mobility, particularly in its nonpolar side chains, as compared with other proteins. These results were consistent with those presented by others, as in sequence predictions (Gray et al., 1973) and optical methods (Debelle and Alix, 1995; Debelle et al., 1995, 1998).

Elasticity in vertebrate tissue appears to be affected by various environmental factors, such as humidity and temperature. Gotte and coworkers measured dynamic-mechanical and other physical properties and found that the elastic fiber and elastin strongly resemble rubber in certain conditions but that the rubbery nature is lost upon dehydration (Gotte et al., 1968). These observations might call into question the role of water in determining the complete picture of elastin structure. Namely, does water play an integral role in the accurate structural determination of elastin, and if so, what is that role? Indeed, bulk and interfacial properties are examined in model systems of rubber elasticity using synthetic polymers and water (Khongtong and Ferguson, 2001). Elastin appears to be similar to its nonbiological counterparts, as various models for this biopolymer have included water as an essential element of the fully functional elastic fiber (Gray et al., 1973; Li et al., 2001; Weis-Fogh and Andersen, 1970).

In fact, Ellis and Packer found strong evidence for the presence of three types of water in hydrated elastin and the elastic fiber (Ellis and Packer, 1976). Results of their ^1H and ^2D NMR studies suggested that the majority of the water molecules are contained in the bulk water that surrounds the fiber. In addition, there are tightly bound, or integral, water molecules. The third type of water is contained in spaces within the bulk elastin. This population of highly mobile, highly localized waters is believed to play a key part in hydrophobic hydration processes, and it is thought to be acutely involved in the elastic function of this protein.

Others have hypothesized that stretched and relaxed elastin have different degrees of hydration at the molecular level (Gray et al., 1973). Again, the role of water appears to play a pivotal role in the definition of structure-function relationships of elastin.

Our studies on elastin isolated from bovine nuchal ligament show that there are significant differences in the solid-state NMR spectra of hydrated and lyophilized elastin. To probe the effects of varied sample conditions, we observed the similarities and differences in ^{13}C CPMAS spectra for samples with 0–100% hydration levels. These results were indicative of major structural changes that occur as

Submitted July 9, 2001, and accepted for publication October 22, 2001.

Address reprint requests to Dr. Kristin K. Kumashiro, Department of Chemistry, University of Hawaii, 2545 McCarthy Mall, Honolulu, HI 96822. Tel.: 808-956-5733; Fax: 808-956-5908; Email: kristin@gold.chem.hawaii.edu.

0006-3495/02/02/1086/10 $2.00

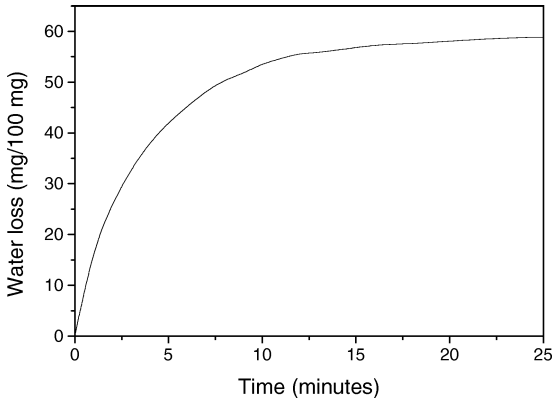

FIGURE 1 Dehydration of elastin using lyophilization. Plot depicts amount of water removed for each 100 mg of wet elastin used, as a function of time on lyophilizer.

approximately two-thirds of the water is removed and/or as the sample temperature is dropped well below the freezing point of water. In addition to striking differences in the resolution and signal-to-noise ratios of the spectra, relaxation measurements support the idea that mobility in the hydrated sample is markedly higher than that of the dehydrated and/or cooled elastin.

MATERIALS AND METHODS

Preparation of elastin sample

Insoluble elastin was purified from bovine nuchal ligament. The tissue is cut into pieces of 1–2 mm diameter. Cyanogen bromide (CNBr) (Aldrich, Milwaukee, WI) is dissolved in 70% formic acid to a CNBr concentration of 50 mg/ml. The solution is deoxygenated by bubbling nitrogen through it. The pieces of tissue are placed in a capped tube previously flushed with nitrogen. One milliliter of CNBr/formic acid solution is added for each 10–30 mg wet weight of tissue. This mixture is left for 24 h, with occasional shaking, in the fume hood. After the digestion is complete, 3–4 vol of water are added, and then these tubes are left uncapped, in the fume hood, for an additional 3–4 h. After centrifugation, the supernatant is discarded, and the pellet, or remaining solid material, is washed with water. This procedure typically gives elastin at ~90% purity. To remove the remaining contaminants, the pellet is extracted with 5 M guanidine chloride with 0.01% dithiothreitol for 24 h followed by extensive washings with warm water (80°C). Purity is assayed by amino acid analysis.

Elastin samples with varying degrees of hydration were prepared as follows. The fully hydrated sample was used directly after the preparative scheme described above. The wet sample was blotted with Kimwipes to remove excess water due to swelling. At this stage, the sample is considered 100% hydrated. Using lyophilization, it was determined that the water content of 100% hydrated elastin was ~60% by mass, which is consistent with measurements of others (Ellis and Packer, 1976; Gotte et al., 1968). Fig. 1 shows a typical curve obtained for a hydrated elastin sample, whereby the sample mass was recorded as a function of time on the lyophilizer. The sample size observed for Fig. 1 was 100 mg per vial (5-ml size). Three vials were placed in the lyophilizer, and Fig. 1 shows the average of the three masses over time. Most of the water (>95%) was removed after 15 min on the lyophilizer. Lyophilization for up to 48 h subsequently will remove only an additional 1–3 mg, or 1–3%, of total sample mass. The sample lyophilized for 48 h is referred to as being 0% hydrated. CPMAS spectra for a sample lyophilized for the additional 2 days are identical to the sample we call 0% hydrated. Partially hydrated samples were obtained by removing samples, after 20 s to 10 min of lyophilization, recording the mass and packing immediately (note 150 mg of sample was used to ensure enough material to fill rotor). Degree of hydration was calculated on the basis of 100% hydration being equal to 60% water by mass. Losses due to handling, such as packing the rotor, were determined to be limited to less than 3%.

NMR spectroscopy

Data were acquired on a Varian Unity Inova WB 400 spectrometer, equipped with a 4-mm double-resonance MAS probe (Chemagnetics, Fort Collins, CO). Rotors were sealed from moisture with a top spacer machined from Kel-F and fitted with fluorosilicone micro o-rings (Apple, Lancaster, NY) (K. W. Zilm, personal communication). Fluorinated polymers were used for reduced ^{13}C background in CPMAS experiments. O-ring seals are necessary to maintain hydration levels during data collection. Protein samples in rotors without seals will dehydrate (or adsorb moisture from the ambient environment) during the course of the NMR experiment, whereas samples in o-ring-sealed rotors show negligible changes in hydration level (as determined by mass). Typical sample sizes used were 64–68 mg and 34–36 mg for the 100% and 0% hydrated samples, respectively.

For cross-polarization, a 5.0-μs ^{1}H 90° pulse was followed by a 1-ms contact time with a 5-s recycle delay. For direct polarization, a 5.0-μs ^{13}C 90° pulse was used with a 20-s recycle delay. Typical applied field strengths for high-power continuous-wave decoupling during acquisition were $\gamma B_1/2\pi = 70–80$ kHz. The spinning speed used in MAS experiments was 8 kHz. Chemical shifts are referenced to the tetramethylsilane scale, using hexamethylbenzene as an external standard.

^{13}C T_1 values were obtained by the method of Torchia (1978). To obtain ^{1}H $T_{1\rho}$ values, a modified cross-polarization pulse sequence was utilized, whereby a ^{1}H spin-locking pulse (0–10 ms) was applied after the ^{1}H 90° pulse and before the CP mixing pulse. The resolved ^{13}C H spin H peak intensities were plotted as a function of time, and the data were fit to a single-exponential decay function.

Data for the wet, dry, and partially dehydrated samples were acquired at −20°C, 4°C, 23°C, and 37°C. More extensive variable-temperature data for the fully hydrated (wet) sample were also acquired at −10°C, −4°C, 0°C, and 15°C.

RESULTS AND DISCUSSION

^{13}C CPMAS of elastin samples with different hydration levels at room temperature

Samples of hydrated and partially and fully dehydrated elastin were prepared. The hydrated elastin sample is 60% water (w/w), and this level of hydration will be referred to as 100% hydrated in this work. This determination of the water content of a typical hydrated, or wet, elastin sample is consistent with the measurements of others. In addition, samples of partially hydrated elastin were prepared with water content ranging from 10% to 90% (w/w), whereby percentages are relative to the 100% hydrated sample. Finally, elastin that has been lyophilized until no further loss of water is measured is dry, or 0% hydrated. It is expected that some small amount of water molecules remain on the protein, and these tightly bound waters cannot be removed by lyophilization.

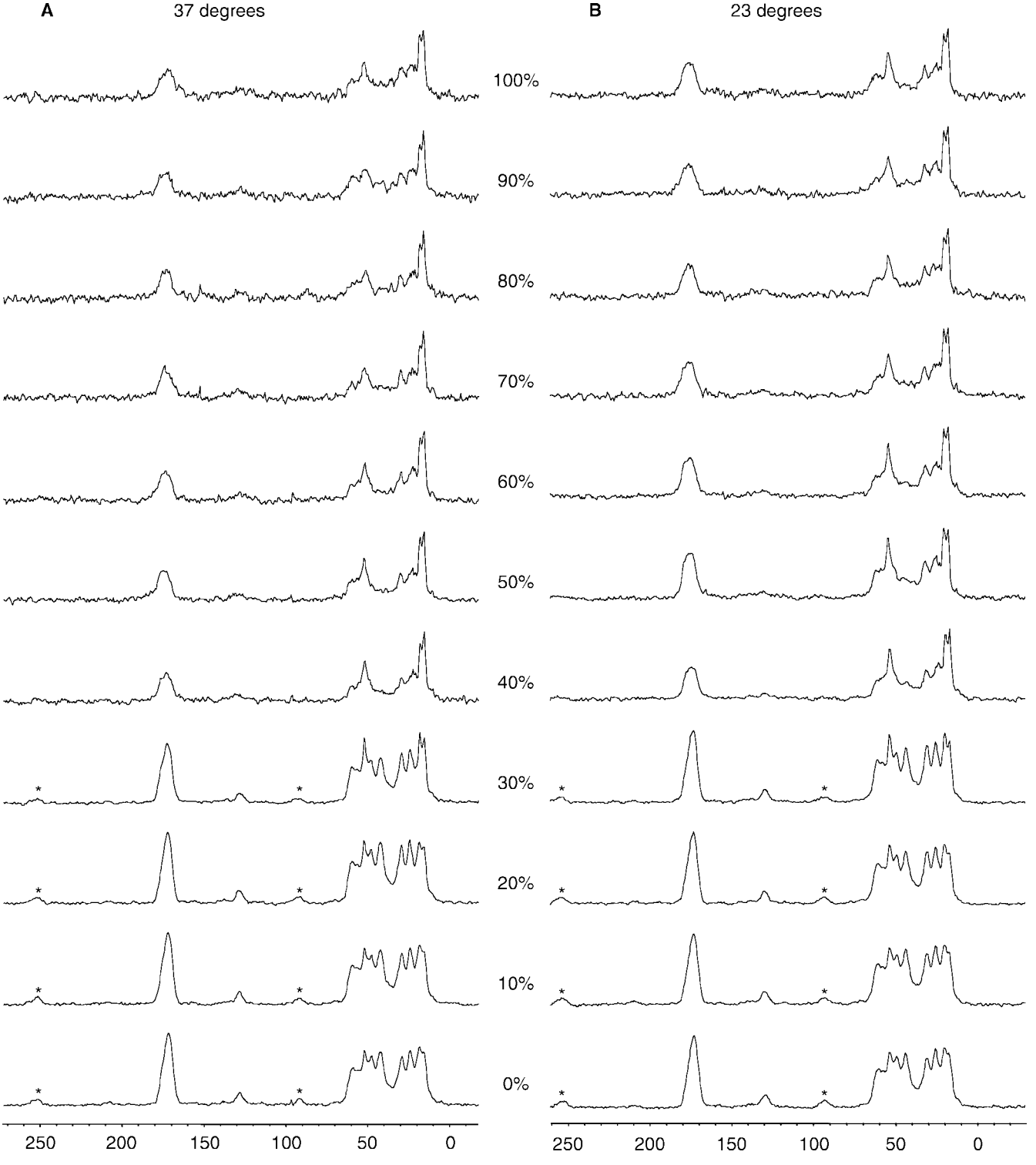

FIGURE 2 ^{13}C CPMAS spectra of elastin with hydration levels of 0–100%. (*A–D*) Data of the 11 samples at 37°C, 23°C, 4°C, and −20°C, respectively. Asterisks indicate spinning sidebands.

Figs. 2, *A–D*, are ^{13}C CPMAS spectra acquired for a series of elastin samples at 37°C, 23°C, 4°C, and −20°C, respectively. Initially, we describe the data in Fig. 2 *B*, acquired at room temperature. The top and bottom traces are the spectra acquired for the wet and dry elastin samples, respectively. As noted, the CPMAS spectra acquired for samples that were partially dehydrated (10%, 20%, 30%, etc) are also illustrated.

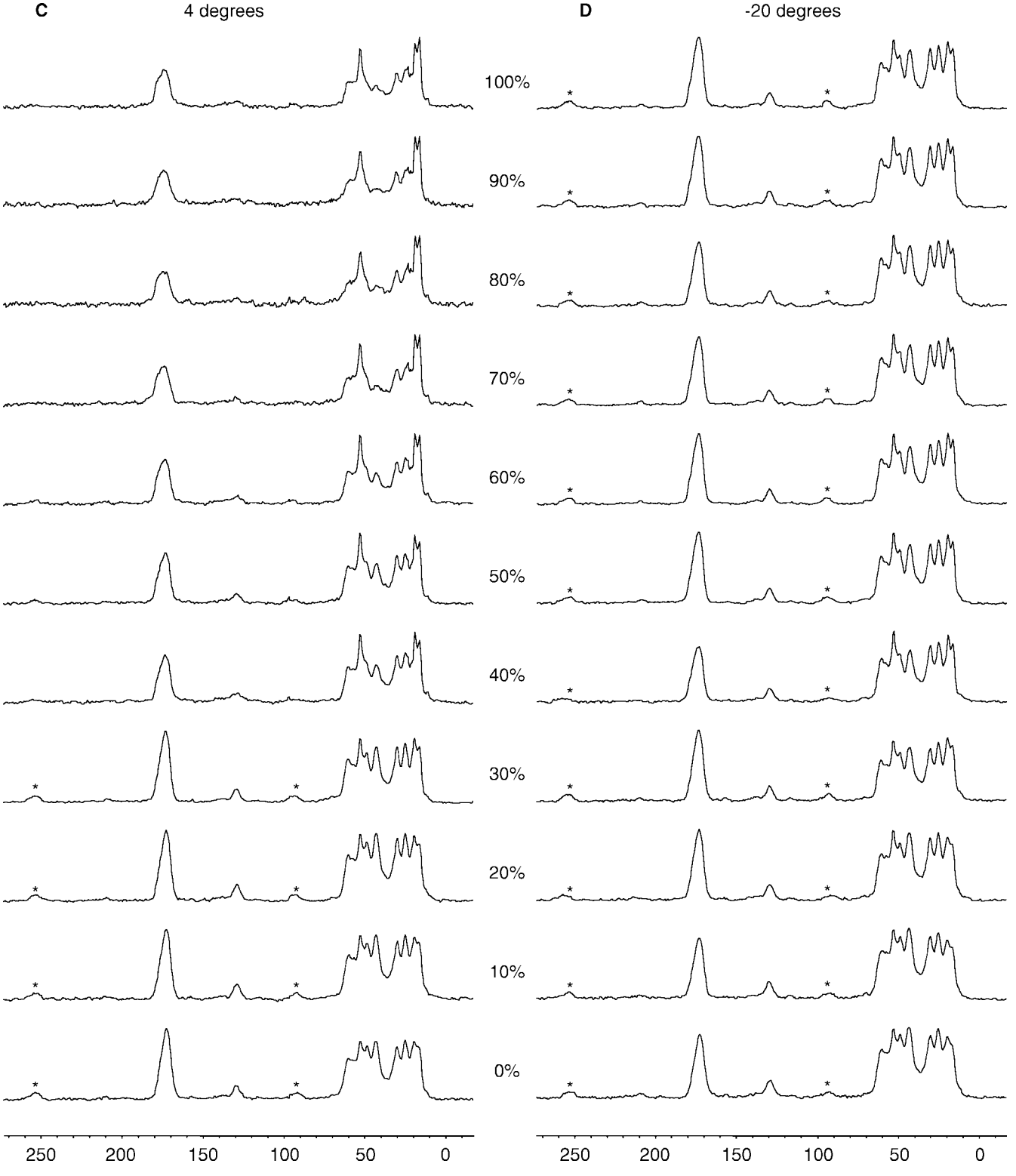

The spectrum of wet elastin shows a broad resonance in the backbone carbonyl region centered at 173 ppm, with a significant linewidth (FWHM ~1 kHz). This linewidth is not unexpected, due to the composition of this biopolymer. The chemical shift of the center of mass of this peak is consistent with that observed for other similar proteins, such as spider silk, with its predominance of Ala and Gly. And our previous work on a lyophilized elastin peptide preparation showed a backbone peak with a nearly identical chemical shift (Kumashiro et al., 2001).

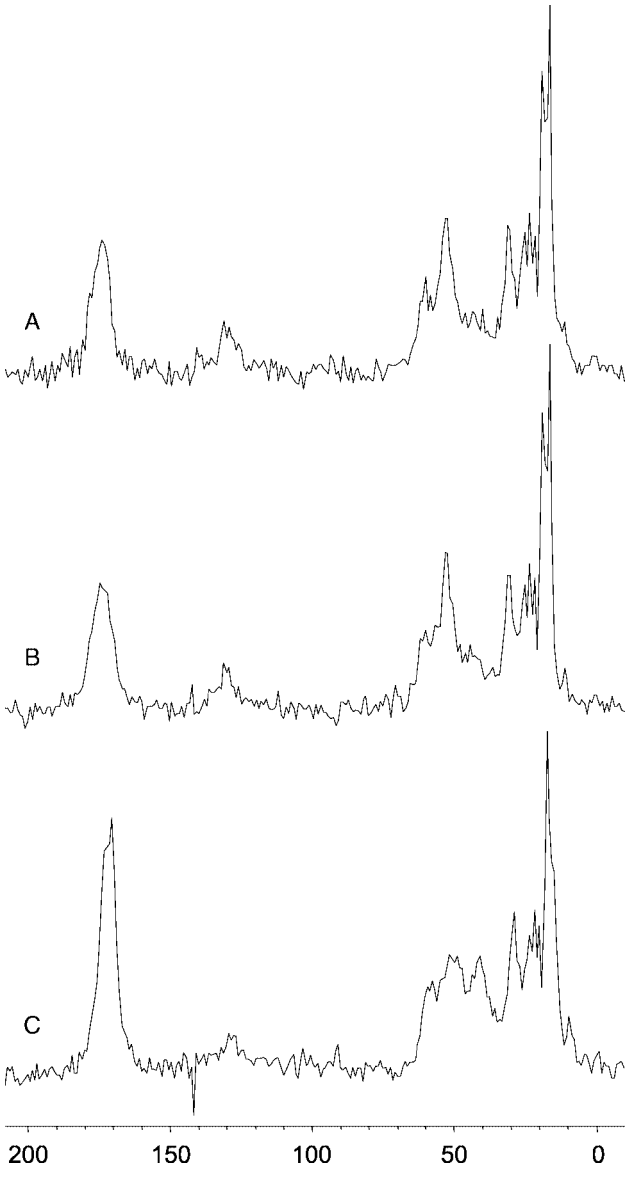

FIGURE 3 (*A*) The ^{13}C CPMAS spectrum of the wet (100% hydrated) elastin with 4000 scans; (*B*) The ^{13}C CPMAS spectrum of the rehydrated sample, taken for a sample of elastin that was lyophilized and subsequently swollen in water for 48 h; (*C*) The DPMAS spectrum of hydrated elastin taken with direct polarization of ^{13}C with decoupling during acquisition. To obtain this information, DPMAS spectra are recorded for the elastin sample as well as an empty rotor. A difference spectrum is shown to remove the background from, e.g., the rotor inserts and other carbon-containing materials.

In addition, there are resonances in the aliphatic region for the fully hydrated elastin. The lineshape in the C^{α} region is dominated by the peak at 53 ppm, and there are resolvable features in the more upfield region. Fig. 3 *A* is a spectrum of the hydrated elastin accumulated with more scans. With more accumulated signal, it is ascertained that there are features that are resolved at 30.9, 25.4, 23.4, and 21.9 ppm. Of the latter three, these peaks are usually observed as a singular, broader feature centered at ~24–25 ppm, depending on the hydration levels. The peaks in the 20–30-ppm region are due to other aliphatic (nonmethyl) side-chain carbons, such as the C^{β}, C^{γ} of valines and prolines. Finally, the tallest feature is clearly two resolvable methyl peaks, at 16.5 and 18.8 ppm. These tentative assignments are based on chemical shift information on peptides, structural proteins, and free amino acids, in addition to the results of spectral editing on elastin preparations (Kricheldorf and Muller, 1983; Kricheldorf et al., 1983; Kumashiro et al., 2000; Pretsch et al., 1983; Saito, 1986).

As the water content decreases from 100% to 40%, there are no major changes in the spectra (top seven traces of Fig. 2 *B*). All show similar relative intensities of the backbone carbonyl peak to the major features of the aliphatic envelope. However, at 30% hydration, there is a marked change. The spectra of the 30%, 20%, 10%, and 0% (fully lyophilized) elastin (bottom 4 traces of Fig. 2) are nearly identical. The backbone carbonyl is still centered at ~173 ppm, but the peak has decreased in linewidth (700 Hz) and increased in relative signal intensity. These spectral changes are not fully explained by the increase in protein mass with the dehydrated samples. More striking, there are now eight to nine resolved peaks in the aliphatic envelope. There are peaks at 60, 57, 53, 49, 43, 30, 25, 19, and 16 ppm. The peaks from 43–60 ppm are C^{α} of the amino acids, with the most upfield (43 ppm) assigned to glycine. The peaks at 30 and 25 owe some of their intensity to the predominant valine and proline residues. And, again, the most upfield features, at 19 and 16 ppm, are assigned to the methyl carbons of, primarily, the valine and alanine residues. The methyl peaks are no longer the most predominant feature in this region, as most of the features have comparable intensities. In addition, the aromatic resonance at 129 ppm is clearly visible in the drier samples. Aromatic carbons that do not have adjacent hetero-atoms would be expected in this region. Therefore, based on the data from, e.g., free amino acid chemical shifts and the amino acid composition of elastin, this region, as dominated by the 129-ppm peak, would be assigned to the side-chain carbons of the phenylalanines.

On one end of the range, the spectrum of the fully hydrated elastin sample has relatively low peak heights, or spectral intensities, as compared with those of the samples with little or no water content (30–0% hydration). There are some differences in protein mass in the hydrated and dehydrated samples; in terms of dry mass protein content, the 0% hydration sample contains 36 mg, whereas the 100% sample contains 27 mg. However, the difference in signal is not explained solely by this factor alone. Our results in the next section, using a single sample, show that similar spectra may be seen over a range of temperatures. Using only the data from the samples with different hydration levels, then we might speculate that the markedly different spectra observed for these samples may, in fact, be due to differences

in cross-polarization efficiencies and that the samples with more water (40–100% hydration) are much more mobile than those with fewer water molecules.

As a final note, the spectra of rehydrated elastin appear to be identical to those that were never dehydrated. Fig. 3 *B* shows a spectrum of an elastin sample that was lyophilized and then rehydrated by swelling in water for 24 h at room temperature. This spectrum, when compared with that of the fully hydrated (100% hydrated) sample, shows no appreciable differences, indicating that the conformational changes that elastin undergoes upon dehydration appear to be reversible.

^{13}C CPMAS spectra of the elastin as a function of both water content and temperature

Fig. 2 shows spectra of the 11 samples at 37°C, 23°C, 4°C, and −20°C. The spectra of the 11 samples at 37°C closely resemble the ones at 23°C. There are some differences in the relative intensities of the backbone carbonyl and the 53-ppm peak in the wetter samples, from 40–100%. Specifically, these peaks appear to have greater heights at room temperature, as compared with the same samples observed at 37°C.

As the sample is cooled further to 4°C, there are further increases in signal intensities in the spectra of all the samples, as compared with the higher temperatures. In addition, the appearance of the aliphatic envelope indicates that the samples with 0–30% hydration levels are similar. Furthermore, the wetter samples have similar spectra and, likely, similar structural and dynamical features. Arguably, the samples with 40–50% water may appear to be an intermediary state, as the relative spectral intensities appear slightly better than the wetter samples but not identical to the driest ones. And, with 40–50% water, the nine aliphatic features are not yet resolved at this temperature.

Finally, the samples are observed at −20°C, significantly below the freezing point of water, where all 11 spectra have comparable intensities and are nearly identical in the appearance of all major features in the backbone carbonyl, aromatic, and aliphatic regions.

The spectra for the series of hydrated-to-dehydrated elastin at the various temperatures illustrate two structural features of elastin. First, the samples with little or no water have spectra that are indicative of powders, with less relative mobility and good cross-polarization efficiency across the population of carbons in the protein. For the samples with higher water content, such as the 40–100% hydrated elastin, there is less signal overall, and fewer carbons appear to cross-polarize well. Certainly, the lower signal is not due entirely to a smaller mass of protein, as the lowering of temperature for any given wet sample results in the enhancement of signal, suggesting that elastin is not a rigid protein. And, if increases in relative intensities and the inferred cross-polarization efficiencies are indicative of slower motion, then the 53-ppm peak represents a portion of the α-carbons that is relatively rigid. The backbone carbonyl peak of the wetter samples at higher temperatures also represents a portion of the carbonyl population that is fairly rigid and cross-polarizes well. However, it is clear that the removal of water and/or the lowering of temperature result in the increase of backbone intensity in the 173-ppm peak and in the entire C^{α} region. In other words, if the intensities are indicative of relative motion, then the decreases in temperature and/or water content cause the rigidification of the entire protein's structure. These changes occur as water is frozen and as approximately two-thirds of the water is removed, respectively.

^{13}C CPMAS spectra of the hydrated elastin as a function of temperature

Fig. 4 shows ^{13}C CPMAS spectra obtained for the fully hydrated (100%) elastin as a function of temperature. At higher temperatures, such as room temperature or physiological, the signal intensities or peak heights are relatively small, and fewer peaks are clearly distinguishable. However, as the temperature is lowered, numerous changes are observed. First, features that are not observed in the wet sample at the higher temperatures become apparent when the sample is cooled. For instance, the 43-ppm peak, which is not observed at 37°C to 15°C, is clearly visible at around 0°C, the freezing point of water. And, it becomes more defined as the temperature is dropped further. At the lowest temperature used, all nine features in the aliphatic region are observed here. In addition, the aromatic peak at 130 ppm is clearly visible at the cooler temperatures.

Again, the ^{13}C CPMAS spectrum of hydrated elastin at −20°C closely resembles that of lyophilized elastin at almost any temperature (bottom traces of Fig. 2, *A–D*). Specifically, the backbone carbonyl, the aromatic peak, and the nine typical features of the aliphatic region are nearly identical in chemical shift and relative intensities for a frozen wet sample and the lyophilized one. In Fig. 4, it is clear that the peak heights increase as the temperature is lowered, with the greatest observed at −20°C. The same sample was used to record all the spectra shown in Fig. 4, thereby demonstrating that accumulated signal is not solely a function of sample size. Thus, it is reasonable to suggest that the increase in signal intensities at the lower temperatures is indicative of a concurrent increase in cross-polarization efficiencies. That is, these spectra strongly suggest that there is a rigidification of the protein as the sample is cooled to temperatures below the freezing point of water. Clearly, the structural change does not occur at the freezing point of water, as the temperature of the sample must be lowered to −20°C to obtain the spectrum that most closely resembles that of the lyophilized elastin.

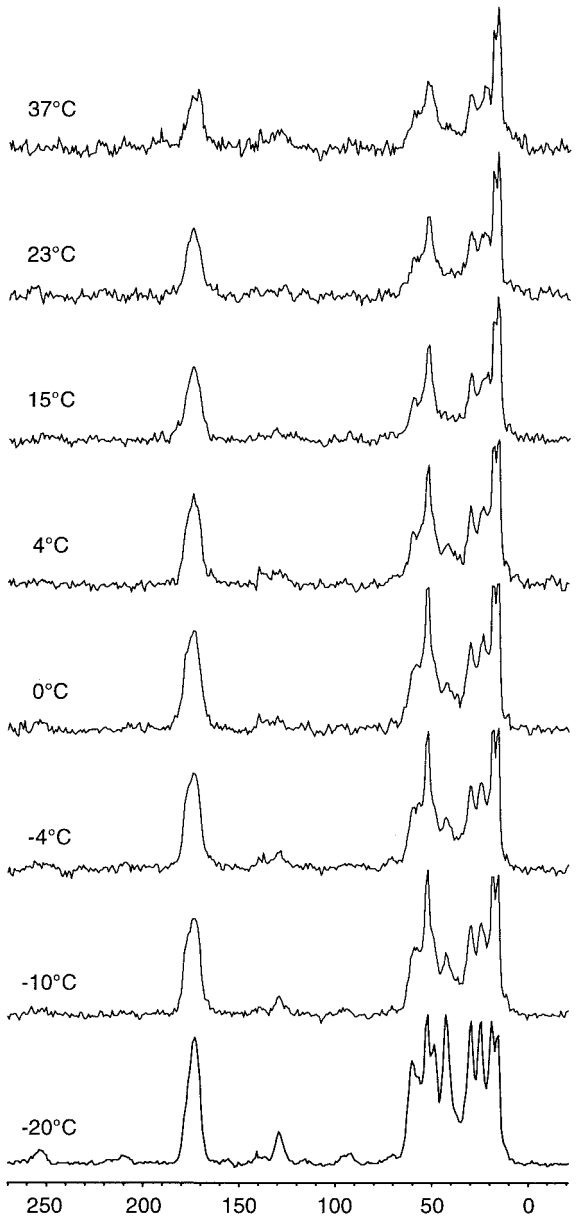

FIGURE 4 Variable-temperature ^{13}C CPMAS spectra of wet (100% hydrated) elastin.

^{13}C DPMAS spectra of hydrated elastin

Cross-polarization efficiencies are not uniform over the population of carbon nuclei in a sample. The number of directly bonded protons and the relative mobility of the carbons are two significant factors that may mediate or mitigate the efficiency of polarization transfer. To identify the population of carbons that do not cross-polarize well, single-pulse excitation with high-power decoupling and magic-angle spinning is used. This experiment is also known as direct polarization with magic-angle spinning (DPMAS). Fig. 3 *C* is a spectrum of hydrated elastin, which was obtained by subtracting the DPMAS spectrum of an empty rotor (with inserts) from that of the one with sample to remove the background signals. For contrast, the ^{13}C CPMAS of the hydrated sample recorded at 37°C is shown in Fig. 3 *A*.

There are several notable differences between the CPMAS and DPMAS of the hydrated elastin. Most striking is the difference in relative peak intensities of the backbone carbonyl and C^{α}-Gly (43-ppm) peaks. In the CPMAS spectra, the backbone carbonyl peak has comparable intensity to, e.g., the 53-ppm peak. In the DPMAS, the height of the backbone peak is at least twice that of any carbon in the C^{α} region. There are also differences in the appearance of the backbone carbonyl feature. In the DPMAS, the backbone carbonyl peak has its tallest point at 172.5 ppm, similar to the CPMAS spectra. However, also clearly visible is a downfield component centered at 175 ppm. Most of the amino acids, with the most notable exception of glycine, have downfield chemical shifts observed for residues in α-helices. This observation indicates that there is a population of mobile backbone carbonyls with resolvable, different environments or secondary structures, possibly in α-helices.

In addition, the 43-ppm peak, assigned to the α-carbon of glycine, is also clearly visible in the DPMAS spectra. Again, this result is indicative of the high relative mobility of the glycines, which would, in turn, not cross-polarize well. Incidentally, it is the 43-ppm peak that becomes visible as hydrated elastin is frozen, as noted in the previous section of this paper.

^{13}C static CP spectra of hydrated and lyophilized elastin

Fig. 5 shows the ^{13}C spectra of hydrated (Fig. 5 *A*) and lyophilized (Fig. 5 *B*) elastin taken with cross-polarization and high-level decoupling during acquisition, but without spinning. The purpose of this variation is the identification of carbons that cross-polarize. Unlike the typical ^{13}C CPMAS experiment, however, the line-narrowing effects of magic-angle spinning are not utilized. The decoupling during acquisition will remove most of the (heteronuclear) dipolar couplings between carbons and protons, but the broadening due to chemical shift anisotropy will be observed in a typical rigid organic solid.

The static pattern for the lyophilized elastin is typical for a dried protein. The broadest lineshape is furthest downfield, and it is representative of the typically large chemical shift anisotropies observed for carbonyl carbons. The more upfield component represents the aliphatic (including methyl) carbons, with their typically smaller anisotropies.

The static CP spectrum of the hydrated sample, however, is atypical for a rigid solid. It has both narrow and broad features, as seen in the backbone carbonyl region. The two identifiable narrow features have chemical shifts of 175 and 170 ppm. These peaks represent a mobile fraction of the

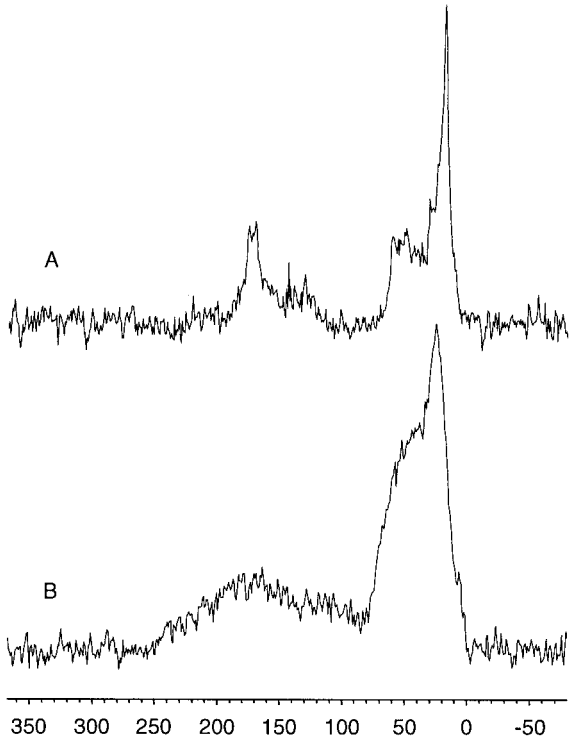

FIGURE 5 The ^{13}C spectrum recorded with cross-polarization and without spinning (static) for hydrated (*A*) and lyophilized (*B*) elastin.

backbone carbonyls, whereby the line narrowing is due to motional effects. Presumably, these peaks are obscured in the CPMAS and DPMAS by the isotropic lineshape for the broader component in the fast-spinning limit. The aliphatic envelope also has narrow features immediately attributable to the methyl carbons. Again, the linewidths of this methyl peak at 18.5 ppm is smaller (200–300 Hz FWHM) than that observed for the static lyophilized protein (~1 kHz). Again, these results are consistent with those for experiments described above; i.e., there is significant mobility in the hydrated elastin samples at physiological temperatures.

Interestingly, it is noted that it is extremely uncommon to observe nuclei in the solid state that will cross-polarize yet exhibit line narrowing reminiscent of motional effects. To investigate the potential for Overhauser effects in this very mobile solid, an experiment was utilized whereby ^{1}H irradiation of various times was applied to the hydrated elastin sample. Then, single-pulse excitation of the ^{13}C was followed by detection with decoupling during acquisition. If there were Overhauser effects, then the ^{13}C peak intensities would increase as the ^{1}H irradiation times (before ^{13}C excitation) increase. For ^{1}H irradiation times of 100 μs, 500 μs, 1 ms, 1.5 ms, and 2.0 ms, most of the spectrum does not change. The only region that displays any type of change is the methyl feature, with only a small peak intensity increase of ~10%.

TABLE 1 ^{13}C T_1 values (in seconds) determined for sites in hydrated and lyophilized elastin

δ	Hydrated		Lyophilized	
(ppm)	−20°C	37°C	−20°C	37°C
16	0.3 ± 0.1	0.4 ± 0.1	0.4 ± 0.1	0.4 ± 0.1
19	0.4 ± 0.1	0.4 ± 0.1	0.5 ± 0.1	0.6 ± 0.1
25	2.3 ± 0.5	0.3 ± 0.2	3.6 ± 0.8	2.1 ± 0.4
30	3.6 ± 0.3	—	5.7 ± 0.4	3.3 ± 0.6
43	6.3 ± 0.4	—	10.0 ± 0.6	6.8 ± 1.3
49	6.4 ± 0.3	—	9.1 ± 0.7	7.8 ± 1.2
53	9.7 ± 0.8	0.3 ± 0.3	13.3 ± 0.4	12.3 ± 2.0
57	9.8 ± 0.9	—	16.1 ± 1.0	12.3 ± 2.7
60	8.5 ± 0.7	—	18.1 ± 2.2	12.2 ± 3.3
129	21.2 ± 8.8	—	15.5 ± 4.5	—
173	17.6 ± 1.2	9.7 ± 2.4	23.2 ± 2.4	30.2 ± 16.4

Measurements were made at physiological (37°C) and low (−20°C) temperatures.

^{13}C T_1 and ^{1}H $T_{1\rho}$ measurements of hydrated and lyophilized elastin

Relaxation measurements, such as determinations of ^{13}C T_1 and ^{1}H $T_{1\rho}$ values of the resolved carbons, are useful in identifying characteristics of the dynamics of the protein.

Table 1 shows ^{13}C T_1 values obtained for the resolved peaks of the hydrated and lyophilized elastin at 37°C and −20°C. As noted in an earlier section, fewer peaks are resolved in the hydrated sample at the higher temperatures. As expected, the methyl peaks have very short time constants, with respect to the rest of the protein, due to the methyl rotor. However, the other resolved peaks in this sample also have short T_1 values, in comparison with those of the frozen hydrated sample and the lyophilized sample at both temperatures. The aliphatic carbons, which include at least one type of α-carbon and the side-chain carbons, have very short T_1 values (<1 s). And the spin-lattice relaxation time for the backbone carbonyl peak, although longer and more characteristic of a solid, is shorter than that observed for the other three conditions.

The T_1 values for the frozen hydrated sample and the lyophilized elastin (at both temperatures) are more representative for proteins in the solid state (Saito and Yokoi, 1992; Simmons et al., 1994; Wang et al., 1996). The 25- and 30-ppm peaks from the side-chain carbons of Pro and Val have short T_1 values on the order of 2–6 s. The α-carbons, with chemical shifts from 43 to 60 ppm, have longer spin-lattice relaxation times, with trends toward larger values for the downfield α-carbons. The 43- and 49-ppm peaks have similar T_1 values for a particular sample at a given temperature. As noted earlier, the peaks at 43 and 49 ppm are tentatively assigned to C^{α}-Gly and C^{α}-Ala, based on literature values for similar proteins and peptides (Simmons et al., 1994; Wang et al., 1996). These two peaks have T_1 = 6.3–6.4 s for the hydrated sample at −20°C. The 43- and 49-ppm peaks have longer relaxation times in the lyophi-

lized sample at 37°C (~7–8 s) and −20°C (~9–10 s). In contrast, the downfield α-carbons have slightly longer relaxation times for each of these three samples; the frozen hydrated sample has T_1 values of 9–10 s, whereas they are ~12–18 s in the lyophilized sample. This small difference hints at a model where glycines and alanines reside in a more mobile environment, even in the absence or freezing of the waters of hydration.

Overall, however, these differences among the frozen hydrated and the lyophilized samples are subtle, and they are shown to highlight the similarities among samples where water has been removed, either by lyophilization or by a phase change. The differences in relaxation behavior observed between hydrated elastin at 37°C and the other three data sets are not unexpected, as the CPMAS data clearly illustrate the similarities between the spectra of the lyophilized elastin and those of the frozen hydrated one.

Interestingly, the T_1 values of the wet sample at 37°C, particularly in the aliphatic region, have nearly liquid-like values. One obvious interpretation of the T_1 results might be that frozen (wet) and lyophilized elastin have rigidified structures, as compared with the wet sample observed at physiological temperatures. They are also consistent with a structural model of elastin with a relatively mobile population, of which glycine comprises a significant amount.

Interestingly, recent solid-state NMR investigations of super-contracted spider silk, an Ala- and Gly-rich protein, have yielded somewhat analogous results to ours (Yang et al., 2000). Spider silk, when wetted, adopts its super-contracted morphology with viscoelastic properties similar to other rubbery materials (Gosline et al., 1984). Namely, the most elastic form of major ampullate silk shows significant mobility, with the hydration levels associated with super-contraction (Yang et al., 2000). T_1 measurements for the carbons in the protein were found to be <1 s, identical to our measurements. And, using the same assumptions as done with the spider silk investigations, we might also infer that the motions of the protein were occurring on the timescale of 10^{-8} s.

TABLE 2 ^{1}H $T_{1\rho}$ values (in msec) determined for sites in hydrated and lyophilized elastin

δ	Hydrated		Lyophilized	
(ppm)	−20°C	37°C	−20°C	37°C
16	5.6 ± 0.8	1.2 ± 0.1	4.9 ± 0.3	9.3 ± 0.5
19	5.3 ± 0.7	1.2 ± 0.1	4.7 ± 0.2	8.9 ± 0.5
25	5.5 ± 0.8	0.8 ± 0.1	4.9 ± 0.3	8.9 ± 0.4
30	5.6 ± 0.8	0.6 ± 0.1	4.8 ± 0.2	8.9 ± 0.3
43	5.6 ± 0.8	—	4.6 ± 0.2	8.4 ± 0.3
49	5.6 ± 0.8	—	4.7 ± 0.2	8.5 ± 0.3
53	6.1 ± 0.9	0.7 ± 0.1	4.9 ± 0.2	8.7 ± 0.4
57	5.8 ± 0.8	—	4.4 ± 0.3	8.6 ± 0.3
60	5.5 ± 0.7	—	4.2 ± 0.2	8.2 ± 0.7
129	5.3 ± 0.8	—	2.2 ± 0.6	3.8 ± 0.7
173	4.9 ± 0.5	0.9 ± 0.1	3.9 ± 0.4	10.0 ± 0.7

Measurements were made at physiological (37°C) and low (−20°C) temperatures

Table 2 shows ^{1}H $T_{1\rho}$ values determined for the wet and dry elastin samples at the two temperatures. Again, it is also clear that the frozen wet sample and the dry sample at either temperature bear similar characteristics. Specifically, all resolved aliphatic carbons have nearly identical ^{1}H $T_{1\rho}$ values, suggesting similar relaxation mechanisms in the hydrophobic regions in elastin, for samples where the interactions between the protein and water have been altered from physiological conditions. In the frozen hydrated sample, the observed ^{1}H $T_{1\rho}$ values are 5–6 ms. In the lyophilized sample at the lower temperature, homogeneous time constants of 4–5 ms across the sample are also observed. As the temperature is raised to 37°C, the relaxation times for, particularly, the aliphatic region increase to 8–9 ms. In contrast, the hydrated sample at 37°C has ^{1}H $T_{1\rho}$ of ~1 ms for all resolved carbons. As with the ^{13}C T_1 values, the measured relaxation times are significantly shorter than those observed for the other samples. And it is clear that the relaxation mechanisms in hydrated elastin proceed differently than either the frozen or anhydrous elastin.

The homogeneity in the ^{1}H $T_{1\rho}$ values indicate that there are no significant heterogeneities in the structural organization of this biopolymer; i.e., the relaxation mechanisms, whether dipole-dipole or otherwise, are fairly uniform across the whole sample. There is some indication that there may be a somewhat different relaxation mechanism for the side-chain aromatic carbons (129 ppm) in lyophilized elastin; it is interesting to note that hydration levels and temperature affect cross-polarization efficiencies and relaxation behavior of these sites, as they do with the aliphatic region of the protein.

Concluding remarks

Our results show that the spectra of elastin depend on sample conditions. Our approach investigated the effects of two parameters, temperature and water content. When a wet sample was cooled well below the freezing point of water, there was a change in the number of resolvable peaks as well as an accompanying change in signal intensities. We indicated that this result was not unexpected, as it might be surmised that the freezing of water would lead to a reduction in protein mobility, particularly if water plays an integral role in the structure and function of the protein. In fact, our results strongly suggest that water does play an integral role in the structure of hydrated elastin, such as in an extensive hydrogen-bonding network whereby waters are not part of a discrete phase.

We observed 11 samples, with water contents of 0–100%. The same overall trends were observed at different temperatures; i.e., more signal intensity was observed at lower temperatures. Furthermore, the protein samples with little or no water were nearly identical, and the spectra of

these drier protein samples resembled that of the frozen wet (100% hydrated) elastin. Again, one might speculate that water must play an integral role in the structure-function of elastin; if the water is frozen so that there is loss of mobility in both the protein and the hydration layers and/or if water is removed, then the elastin adopts an energetically favorable configuration that excludes interactions with surrounding water molecules.

In addition to the spectral differences already described, it is interesting to note that hydrated elastin may be dehydrated to the point where nearly two-thirds of its water is removed and the spectra remain nearly unchanged. Specifically, the CPMAS spectra of the 0–30% hydrated elastin are similar, and samples with 40–100% hydration are reasonably close in appearance as well. Interestingly, the physical properties of elastin exhibit a nearly identical relationship to hydration. Namely, samples with 40–100% hydration have rubber-like characteristics of flexibility and elasticity, whereas samples with 0–30% hydration are brittle. Specifically, the work of Gotte and coworkers showed that the elastic modulus of elastin changes dramatically when two-thirds or more of the water is removed (Gotte et al., 1968).

Our result may lend further support toward the existence of a localized water phase. That is, the first 60–70% of the water removed may belong to a bulk water phase, held least tightly to the protein, whereas the last third represents a group of waters held more tightly to the protein, perhaps through direct hydrogen bonding with the elastin. Indeed, this picture is consistent with the work of Ellis and Packer (1976), who discussed such a distribution based on their relaxation measurements, and with the calculations of Daggett and coworkers (Li et al., 2001). These earlier studies indicated that the first hydration shell of elastin would correspond to an ~30% hydration level. As water is added, one plausible model might include an extensive hydrogen-bonding network from peptide backbone to H_2O molecules in the first, second, and subsequent hydration shells. And the dynamic nature of the bulk water might lend significant mobility to the protein, particularly if the two are effectively coupled.

As a final note, our work on the structure-function relationships is ongoing. As we have identified two of the most sensitive parameters for characterization of biologically relevant elastin, we now work toward eliminating yet more of the spectral ambiguities, particularly as they relate to site-specific or residue-specific information for this unique biopolymer.

We thank W. P. Niemczura and S. E. Kaczmarek for technical assistance and L. B. Sandberg for amino acid analyses. Dr. Niemczura is also acknowledged for helpful discussions and critical reading of this manuscript. K. K. Kumashiro gratefully acknowledges support from the CAREER Program of the National Science Foundation (MCB-9733035).

REFERENCES

Debelle, L., and A. J. P. Alix. 1995. Optical spectroscopic determination of bovine tropoelastin molecular model. *J. Mol. Struct.* 348:321–324.

Debelle, L., A. J. P. Alix, M.-P. Jacob, J.-P. Huvenne, M. Berjot, B. Sombret, and P. Legrand. 1995. Bovine elastin and kappa-elastin secondary structure determination by optical spectroscopies. *J. Biol. Chem.* 270:26099–26103.

Debelle, L., A. J. P. Alix, S. M. Wei, M.-P. Jacob, J.-P. Huvenne, M. Berjot, and P. Legrand. 1998. The secondary structure and architecture of human elastin. *Eur. J. Biochem.* 258:533–539.

Ellis, G. E., and K. J. Packer. 1976. Nuclear spin-relaxation studies of hydrated elastin. *Biopolymers.* 15:813–832.

Gosline, J. M., M. W. Denny, and M. E. DeMont. 1984. Spider silk as rubber. *Nature.* 309:551–552.

Gotte, L., M. Mammi, and G. Pezzin. 1968. Some structural aspects of elastin revealed by x-ray diffraction and other physical methods. *In* Symposium on Fibrous Proteins. Butterworths, Sydney, Australia. 236–245.

Gray, W. R., L. B. Sandberg, and J. A. Foster. 1973. Molecular model for elastin structure and function. *Nature.* 246:461–466.

Khongtong, S., and G. S. Ferguson. 2001. Integration of bulk and interfacial properties in a polymeric system: rubber elasticity at a polybutadiene/water interface. *J. Am. Chem. Soc.* 123:3588–3594.

Kricheldorf, H. R., and D. Muller. 1983. Secondary structure of peptides. III. ^{13}C NMR cross polarization/magic angle spinning spectroscopic characterization of solid polypeptides. *Macromolecules.* 16:615–623.

Kricheldorf, H. R., M. Mutter, F. Maser, D. Muller, and H. Forster. 1983. Secondary structure of peptides. IV. ^{13}C-NMR CP/MAS investigations of solid oligo- and poly(L-alanines). *Biopolymers.* 22:1357–1372.

Kumashiro, K. K., M. S. Kim, S. E. Kaczmarek, L. B. Sandberg, and C. D. Boyd. 2001. ^{13}C CPMAS NMR studies of α-elastin preparations show retention of overall structure and reduced mobility with a decreased number of crosslinks. *Biopolymers.* 59:266–275.

Kumashiro, K. K., W. P. Niemczura, M. S. Kim, and L. B. Sandberg. 2000. Selection of side-chain carbons in a high-molecular-weight, hydrophobic peptide using solid-state spectral editing methods. *J. Biomol. NMR.* 18:139–144.

Li, B., D. O. V. Alonso, and V. Daggett. 2001. The molecular basis for the inverse temperature transition of elastin. *J. Mol. Biol.* 305:581–592.

Pretsch, E., J. Seibl, W. Simon, and T. Clerc. 1983. Tables of Spectral Data for Structure Determination of Organic Compounds, English translation of the second German edition. Springer-Verlag, Berlin.

Rosenbloom, J., W. R. Abrams, and R. Mecham. 1993. Extracellular matrix. IV. The elastic fiber. *FASEB J.* 7:1208–18.

Saito, H. 1986. Conformation-dependent ^{13}C chemical shifts: a new means of conformational characterization as obtained by high-resolution solid-state ^{13}C NMR. *Magn. Reson. Chem.* 24:835–852.

Saito, H., and M. Yokoi. 1992. A ^{13}C NMR study on collagens in the solid state: hydration/dehydration-induced conformation change of collagen and detection of internal motions. *J. Biochem.* 111:376–382.

Simmons, A., E. Ray, and L. W. Jelinski. 1994. Solid-state ^{13}C NMR studies of *Nephila clavipes* dragline silk established structure and identity of crystalline regions. *Macromolecules.* 27:5235–5237.

Torchia, D. A. 1978. The measurement of proton-enhanced carbon-13 T_1 values by a method which suppresses artifacts. *J. Magn. Reson.* 30: 613–616.

Wang, J., A. D. Parkhe, D. A. Tirrell, and L. K. Thompson. 1996. Crystalline aggregates of the repetitive polypeptide $\{(AlaGly)_3$-$GluGly(GlyAla)_3GluGly\}_{10}$: structure and dynamics probed by ^{13}C magic angle spinning nuclear magnetic resonance spectroscopy. *Macromolecules.* 29:1548–1553.

Weis-Fogh, T., and S. O. Andersen. 1970. New molecular model for the long-range elasticity of elastin. *Nature.* 227:718–721.

Yang, Z., O. Liivak, A. Seidel, G. LaVerde, D. B. Zax, and L. W. Jelinski. 2000. Supercontraction and backbone dynamics in spider silk: ^{13}C and ^{2}H NMR studies. *J. Am. Chem. Soc.* 122:9019–9025.